Apoptosis (2018) 23:27–40
https://doi.org/10.1007/s10495-017-1434-7

ORIGINAL PAPER

Molecular docking studies of bioactive compounds from *Annona muricata* Linn as potential inhibitors for Bcl-2, Bcl-w and Mcl-1 antiapoptotic proteins

Mohamad Norisham Mohamad Rosdi[1] · Shahkila Mohd Arif[2] · Mohamad Hafizi Abu Bakar[3] · Siti Aisyah Razali[4] · Razauden Mohamed Zulkifli[5] · Harisun Ya'akob[1,6]

Published online: 4 December 2017

Abstract

Annona muricata Linn or usually identified as soursop is a potential anticancer plant that has been widely reported to contain valuable chemopreventive agents known as annonaceous acetogenins. The antiproliferative and anticancer activities of this tropical and subtropical plant have been demonstrated in cell culture and animal studies. *A. muricata* L. exerts inhibition against numerous types of cancer cells, involving multiple mechanism of actions such as apoptosis, a programmed cell death that are mainly regulated by Bcl-2 family of proteins. Nonetheless, the binding mode and the molecular interactions of the plant's bioactive constituents have not yet been unveiled for most of these mechanisms. In the current study, we aim to elucidate the binding interaction of ten bioactive phytochemicals of *A. muricata* L. to three Bcl-2 family of antiapoptotic proteins viz. Bcl-2, Bcl-w and Mcl-1 using an in silico molecular docking analysis software, Autodock 4.2. The stability of the complex with highest affinity was evaluated using MD simulation. We compared the docking analysis of these substances with pre-clinical Bcl-2 inhibitor namely obatoclax. The study identified the potential chemopreventive agent among the bioactive compounds. We also characterized the important interacting residues of protein targets which involve in the binding interaction. Results displayed that anonaine, a benzylisoquinoline alkaloid, showed a high affinity towards the Bcl-2, thus indicating that this compound is a potent inhibitor of the Bcl-2 antiapoptotic family of proteins.

Keywords Apoptosis · Bcl-2 inhibitor · Antiapoptotic proteins · *Annona muricata* Linn · Molecular docking · MD simulation

✉ Harisun Ya'akob
harisun@ibd.utm.my

[1] Department of Bioprocess and Polymer Engineering, Faculty of Chemical and Energy Engineering, Universiti Teknologi Malaysia, 81310 Skudai, Johor, Malaysia

[2] Department of Biotechnology and Medical Engineering, Faculty of Biosciences and Medical Engineering, Universiti Teknologi Malaysia, 81310 Skudai, Johor, Malaysia

[3] Bioprocess Technology Division, School of Industrial Technology, Universiti Sains Malaysia, 11800 Gelugor, Penang, Malaysia

[4] Bioinformatics Research Group, Faculty of Biosciences and Medical Engineering, Universiti Teknologi Malaysia, 81310 Skudai, Johor, Malaysia

[5] Department of Bioscience and Health Sciences, Faculty of Biosciences and Medical Engineering, Universiti Teknologi Malaysia, 81310 Skudai, Johor, Malaysia

[6] Institute of Bioproduct Development, Universiti Teknologi Malaysia, 81310 Skudai, Johor, Malaysia

Introduction

Since the early 1970s, cancer has never failed to amaze, created deep interest among scientific community. This malady remains as one of the most devastating diseases on earth, taking millions of lives every year. In 2012, statistic by World Health Organization (WHO) predicted the rising of cancer mortalities from 7.6 million (2008) to 13 million (2030) [1–4]. Another report estimated a significant rise of cancer cases; approximately 19.3 million new cases per year by 2025, primarily occurs in less developed countries [1, 5, 6]. Cancer can be characterized by several hallmarks including self-sufficiency in growth signals, insensitive to growth inhibitors, tissue evasion and metastasis, unlimited replicative potential, inducing angiogenesis, evasion of apoptosis, genome instability, inflammation, avoiding immune destruction and reprogramming energy metabolism, which have been proposed and well described by Hanahan and

Weinberg [7, 8]. Among them, the ability of cancer cells to evade apoptosis continues to be a crucial attribute of cancer cells.

Mitochondrial intrinsic pathway, a key signaling mechanism in apoptosis, is mainly regulated by a group of proteins known as B cell lymphoma-2 (Bcl-2) family of proteins [9, 10]. This type of proteins consists of antiapoptotic, proapoptotic activators and proapoptotic effectors that in some ways interact with each other to function [11–13]. During apoptosis, activators such as tBid, Puma and Bim, bind to the antiapoptotic and proapoptotic Bcl-2 proteins [14]. The effector proteins including Bad, Noxa, Bik, Hrk, Bnip3 and Bmf, liberate the activators from antiapoptotic proteins (i.e. Bcl-2, Bcl-w, Bcl-XL, Mcl-1 and A1), thus initiating mitochondrial outer membrane permeabilization (MOMP), releasing biomarker such as cytochrome c and apoptosis inducing factor (AIF) [15–20]. Subsequently, this process leads to the initiation of apoptotic machinery.

Impaired apoptosis is crucial in cancer progression. Apoptotic mechanism is mainly inhibited by direct interaction with antiapoptotic protein members; these proteins bind and sequester activators from interacting with effectors, thus directly prevent effectors from activating MOMP [20]. Overexpression of Bcl-2 antiapoptotic proteins has been discovered to prevent apoptosis induced by chemo-drugs in various cancers [21]. The capacity of these proteins to interrupt apoptosis has gained interest for cancer drug development. Bcl-2 antiapoptotic proteins contain BH1, BH2 and BH3 domains by forming the surface-binding hydrophobic pocket which mediates protein–protein interactions involving Bcl-2 family of proteins [22]. Interference in this cleft eradicates the antiapoptotic function of the protein members, indicating its potency. For example, synthetic peptides that interact with hydrophobic pocket of Bcl-2 proteins have been shown to induce apoptosis in vitro [23–26]. Despite the fact that many drugs have been designed for targeting Bcl-2 antiapoptotic protein members in the past few years, it has not produced the beneficial clinical result [27].

Annona muricata Linn contains various bioactive components that could potentially be the candidate for Bcl-2 antiapoptotic proteins inhibitor. This tropical plant has been reported to stimulate apoptosis in various types of cancer cells [28–32]. This activity is regulated by groups of bioactive compounds such as acetogenins and alkaloid. For instance, acetogenins have been shown to induce apoptotic cell death through the inhibition of mitochondrial complex I in hepatocellular carcinoma (HepG2) cells [33]. In the current study, we used in silico molecular docking software to investigate the interaction between several important bioactive constituents of *A. muricata* L. and Bcl-2 antiapoptotic members viz. Bcl-2, Bcl-w and Mcl-1. We systematically characterized and identified interacting residues between protein targets and the compounds. MD simulation was used to evaluate the stability of the complex formed. This paper explores the potential of natural substances from *A. muricata* L. for the development of Bcl-2 antiapoptotic proteins inhibitor.

Materials and methods

Molecular docking analysis

Data preparation

Ten phytochemicals that are present in *A. muricata* L leaves namely bullatacin (**1**), annocatalin (**2**), annomuricin A (**3**), annomuricin B (**4**), annonacin (**5**), anonaine (**6**), coreximine (**7**), annonacinone (**8**), murisolin (**9**) and synpharine (**10**) were selected as ligands. Obatoclax (**11**), a pre-clinical Bcl-2 inhibitor, was used as control ligand. The 3D molecular structures were retrieved from chemical databases namely PubChem and ChemSpider (Table 1). The retrieved files were converted to .pdb file format by using Discover Studio Visualizer 4.0 software (Accelrys Software Inc., San Diego, CA).

The crystal structures of Bcl-2 (PDB ID: 4MAN), Bcl-w (PDB ID: 2Y6W), Mcl-1 (PDB ID: 5FDO) were retrieved from RCSB Protein Data Bank. The files were saved as Target.pdb. Using AutoDock 4.2 software, polar hydrogen atoms and Kollman partial charges were added to the 3D structures. The macromolecule file was written as .pdbqt file format for further analysis.

Docking procedure

Docking calculations were performed using AutoDock 4.2 software [34]. Ligands were docked into the target structures. Grid box values were obtained from numerous number of trial and error. In this study, the grid size were set to

Table 1 List of ligands used in this study

No.	Ligand	PubChem ID	ChemSpider ID
1	Bullatacin	183613	9300122
2	Annocatalin	44566987	8229811
3	Annomuricin A	157682	138751
4	Annomuricin B	44575650	4477504
5	Annonacin	354398	314587
6	Anonaine	160597	141120
7	Coreximine	601259	522694
8	Annonacinone	14456327	317133
9	Murisolin	11399084	9573984
10	Synephrine	7172	6904
11	Obatoclax	16681698	21430401

100 × 100 × 100 points with 0.375 Å spacing centered on Bcl-2, 80 × 118 × 100 points with 0.447 Å spacing centered on Bcl-w and 110 × 100 × 100 points with 0.375 Å spacing centered on Mcl-1. Lamarckian Genetic Algorithm (LGA) was implemented to analyze protein–ligand interactions. The default settings were applied for other parameters. AutoDock tools was used to produce the grid and docking parameter files [35]. Both AutoGrid and AutoDock computations were performed on Cygwin based on the study by Rizvi el. [35]. Ten independent docking runs were completed for each ligand. Docking files were analyzed using AutoDock 4.2 to identify binding energy and inhibition constant of the interactions. The results were compared between bioactive compounds and obatoclax.

Protein–ligand complex analysis

Discovery Studio Visualizer 4.0 was used to analyze and generate illustrations of protein–ligand complexes. The software was also used to analyze and characterize the interaction of docked protein–ligand complex to determine the polar and hydrophobic interactions between ligand and target. The illustrations of such interactions were generated.

Molecular dynamics simulation of Bcl-2 protein ligand complex

Protein model development

Bcl-2 protein sequence was retrieved from UniProt database (accession number; P10415). The model was generated using Phyre2 online server of Imperial College, London (http://www.sbg.bio.ic.ac.uk/phyre2/) [36]. The template for the model was identified from PDB (4MAN) and the sequence alignment of the template and the desired protein was performed using clustalW online server in order to obtain the input for the modeling process.

Protein model validation

The generated 3D protein model was validated using ERRAT [37] and Verify3D [38, 39] by Structural Analysis and Verification Server (SAVES) version 4 of University of California at http://services.mbi.ucla.edu/SAVES/. The stereochemical quality and accuracy of the 3D protein model was assessed using Ramachandran plot analysis [40] using Ramachandran Plot Assessment (RAMPAGE) tool, University of Cambridge (http://morded.bioc.cam.ac.uk/~rapper/rampage.php). The generated 3D protein model was superimposed with its template. The similarity was assessed using UCSF Chimera software [41]. The molecular docking was proceeded with two ligands: anonaine and obatoclax.

Molecular dynamics (MD) simulation and analysis

MD simulation of Bcl-2/anonaine and Bcl-2/obatoclax complexes (docked complexes) were conducted using GROMACS 5.14 software package [42] and GROMOS 54a7 force field [43]. Each of the protein complexes was simulated at 310.15 K. The protein was solvated in cubic box using Single Point Charge (SPC) water molecules. Due to the limitation of GROMACS to parameterize the heteroatom group in PDB file, all ligand topologies were generated using the PRODRG server [44]. The Na^{2+} ions were randomly placed to neutralize the simulation system. The proteins were imposed in periodic boundary condition (PBC) and electrostatic interactions were improved by Particle Mesh Ewald (PME) summation method which was used to treat coulomb potential [45] which is the best method for computing long-range electrostatics. The systems were energy-minimized using 5000 steps from the steepest descent algorithm followed by equilibration for 100 ps pf solute-position-restrained MD. Each system was restrained MD in 2-fs time step using Linear Constrains (LINCS) algorithm for fixing all bond lengths in the system [46]. The equilibrated structures were subjected to MD simulation for 20 ns (20,000 ps). All the resulting trajectories were analyzed based on stability and compactness of the structure. The stability was analyzed by calculating the root mean square deviation (RMSD) of the backbone of protein structure, root mean square (RMSF) of Cα atom, radius of gyration (Rg) and solvent accessible surface area (SASA) of the entire protein using the GROMACS program.

Results

Molecular docking

After the docking procedure, the ligands were ranked according to their protein–ligand binding energies. The results were analyzed based on the interactions between antiapoptotic proteins and the compounds as well as the binding energies of the complexes. In the current study, we found that anonaine and coreximine demonstrated good affinity with the investigated antiapoptotic proteins comparable to obatoclax. Anonaine has shown the significant affinity towards Bcl-2, therefore the stability of the Bcl-2/anonaine and Bcl-2/obatoclax complexes were further analyzed using MD simulation. Results for binding energy (kcal/mol) and inhibition constants were summarized in Table 2.

Table 2 The binding strength of investigated ligands with the antiapoptotic proteins

Protein target	Ligand	Binding energy (kcal/mol)	Inhibition constant
Bcl-2	Bullatacin	−2.65	11.46 mM
	Annocatalin	−2.48	15.11 mM
	Annomuricin A	−1.10	155.51 mM
	Annomuricin B	−2.22	23.77 mM
	Annonacin	−1.99	34.52 mM
	Anonaine	−8.11	1.13 µM
	Coreximine	−7.13	5.91 µM
	Annonacinone	−1.03	176.43 mM
	Murisolin	−2.27	21.85 mM
	Synephrine	−5.09	186.90 µM
	Obatoclax	−7.01	6.51 µM
Bcl-w	Bullatacin	−2.60	12.42 mM
	Annocatalin	−0.83	244.81 mM
	Annomuricin A	−1.69	57.76 mM
	Annomuricin B	−3.78	1.69 mM
	Annonacin	−1.64	62.48 mM
	Anonaine	−6.91	8.66 µM
	Coreximine	−5.80	55.97 µM
	Annonacinone	−1.56	72.06 mM
	Murisolin	−1.85	44.27 mM
	Synephrine	−4.76	324.84 µM
	Obatoclax	−7.24	4.92 µM
Mcl-1	Bullatacin	−1.05	170.24 mM
	Annocatalin	−0.01	979.15 mM
	Annomuricin A	−0.79	264.01 mM
	Annomuricin B	−2.73	10.02 mM
	Annonacin	−0.03	948.57 mM
	Anonaine	−8.82	344.78 nM
	Coreximine	−7.62	2.61 µM
	Annonacinone	−0.77	272.90 mM
	Murisolin	−1.15	142.48 mM
	Synephrine	−4.53	481.17 µM
	Obatoclax	−8.25	898.29 nM

Binding interaction with Bcl-2

The illustration of molecular interaction holding anonaine in the active site is shown in Fig. 1a, b. The docking simulation of Bcl-2 to anonaine resulted in the formation of 11 hydrophobic interactions with an energy of −8.11 kcal/mol and an inhibition constant of 1.13 µM. As shown in Table 2, the binding energy recorded for anonaine was lower than the binding energy of obatoclax (−7.01 kcal/mol). Several hydrophobic amino acid residues in BH1, BH2 and BH3 hydrophobic pocket domains formed interactions with anonaine. These interactions were formed between four different amino acid residues. No hydrogen bond was observed. Five hydrophobic interactions including two Pi-Alkyl, two Alkyl and one Pi-Sigma types of interaction were formed between anonaine and hydrophobic Met-112 residue alone. Another residue that was highly interacted with anonaine was Leu-134, also a hydrophobic amino acid. Two Pi-Sigma and 1 Pi-Alkyl hydrophobic interactions were formed between Leu-134 and anonaine (Table 3).

On the other hand, the protein-docked analysis showed that coreximine has good binding affinity towards Bcl-2 protein. The molecular interactions were shown in Fig. 1c, d. The result demonstrated that coreximine interacted with a binding energy of −7.13 kcal/mol. The energy is slightly lower than the binding energy recorded by obatoclax interaction. Twelve hydrophobic interactions were formed between coreximine and Bcl-2. No hydrogen bond was observed. Similar to anonaine and obatoclax, Met-112 formed three hydrophobic interactions with coreximine including one Pi-Alkyl and two Alkyl type of interaction. Coreximine also formed two interactions with Leu-134 residue. They are one Pi-Sigma and one Alkyl type of interaction. Another residue that was highly formed the interaction is hydrophobic Ala-146, located in BH1 domain. Ala-146 formed three interactions including two Alkyl and one Pi-Alkyl. The results were shown in Table 4.

These results exhibited similarity with obatoclax interactions. Similar residue was also observed to involve in the interaction between obatoclax and hydrophobic binding pocket of Bcl-2 protein. Met-112 in BH3 domain formed three hydrophobic interactions with obatoclax including two Alkyl and one Pi-Alkyl type of interaction. Obatoclax also formed three hydrophobic interactions including one Pi-Sigma and two Alkyl type of interaction with Leu-134 that was located in BH1 domain. Additionally, another hydrophobic amino acid namely Phe-101 located in BH3 formed interactions with obatoclax. Furthermore, four hydrophobic interactions were formed with Ala-146 residue. The results were summarized in Table 5.

Binding interaction with Bcl-w

The interactions between anonaine and residues in Bcl-w were shown in Fig. 2a, b. The binding energy formed was −6.91 kcal/mol which was slightly higher compared to the energy formed between obatoclax interaction (Table 2). No hydrogen bond was formed. However, three hydrophobic interactions were formed involving hydrophobic amino acid residues namely Leu-86 and Val-82. These residues are located in BH1 domain of Bcl-w. Two hydrophobic interactions were formed between Leu-86 and anonaine. They are Pi-Alkyl and Pi-Sigma interactions with distance of 4.88 and 3.84 Å, respectively (Table 3).

The illustration of molecular docking for the interactions of coreximine and Bcl-w was shown in Fig. 2c, d.

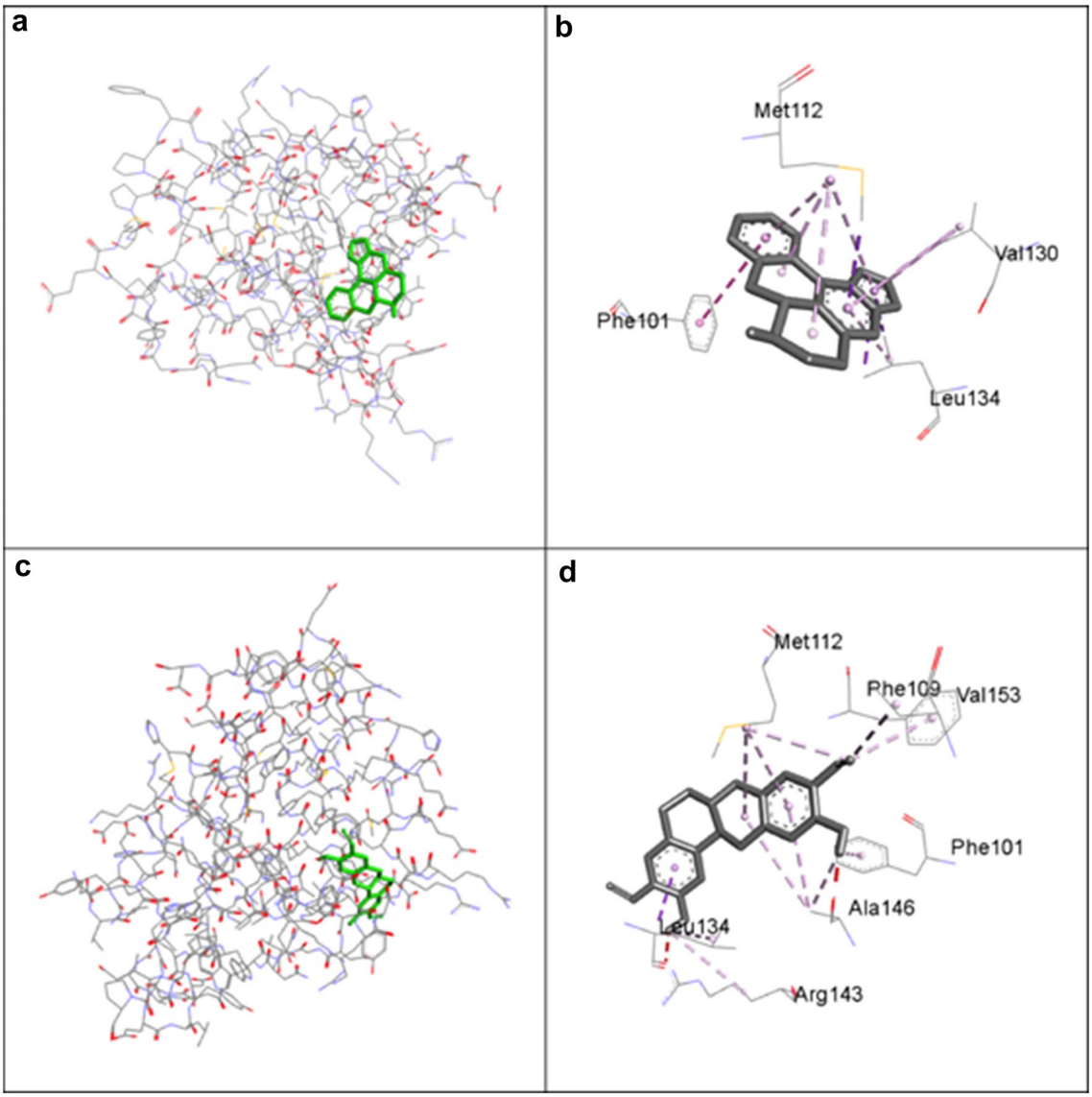

Fig. 1 Binding interactions of anonaine and coreximine in Bcl-2. **a** Representation illustration of anonaine interactions in the hydrophobic pocket of Bcl-2. **b** Hydrophobic interactions of anonaine with residues in the hydrophobic pocket of Bcl-2. **c** Representation illustration of coreximine interactions in the hydrophobic pocket of Bcl-2. **d** Hydrophobic interactions of coreximine with residues in the hydrophobic pocket of Bcl-2

Coreximine formed five hydrogen bonds with five different residues namely Arg-59, Arg-78, Glu-85, Gly-89 and Gly-90 (Table 4). Coreximine also formed five Pi-Alkyl hydrophobic interactions with two different residues namely Val-82 and Arg-56. Glu-85, Gly-89, Gly-90 and Val-82 were located in BH1 domain. The interactions resulted in the binding energy of − 5.80 kcal/mol.

Similarly, obatoclax also formed hydrophobic interactions and hydrogen bonds with BH1 domain. In addition, it also formed interactions with BH2 domain (Table 5).

Binding interaction with Mcl-1

The molecular interactions of anonaine and Mcl-1 residues were shown in Fig. 3a, b. Leu-267 residue in BH1 domain formed three hydrogen bonds with anonaine with length of 2.80, 2.28 and 3.03 Å (Table 3). It has been observed that anonaine formed 11 hydrophobic interactions with nine residues (Table 3). These residues were hydrophobic amino acids located between BH3, BH2 domain and Mcl-1 protein. The interactions resulted in the binding energy of -8.82 kcal/mol comparable to the binding energy of obatoclax (-8.25 kcal/mol) (Table 2).

Table 3 The anonaine interacting residues of the three Bcl-2 antiapoptotic proteins are summarized with the number of hydrophobic interactions and the number of hydrogen bonds

Protein target	Interacting residues	No. of hydrophobic interaction	No. of hydrogen bond
Bcl-2	Phe-101	1	–
	Met-112	5	–
	Val-130	2	–
	Leu-134	3	–
Bcl-w	Val-82	1	–
	Leu-86	2	–
Mcl-1	Met-231	1	–
	Leu-235	1	–
	Val-249	1	–
	Met-250	1	–
	Val-253	2	–
	Leu-267	1	3
	Phe-270	2	–
	Val-274	1	–
	Ile-294	1	–

Table 4 The coreximine interacting residues of the three Bcl-2 antiapoptotic proteins are summarized with the number of hydrophobic interactions and the number of hydrogen bonds

Protein target	Interacting residues	No. of hydrophobic interaction	No. of hydrogen bond
Bcl-2	Phe-101	1	–
	Met-112	3	–
	Leu-134	2	–
	Arg-143	1	–
	Ala-146	2	–
	Val-153	1	–
Bcl-w	Arg-56	2	–
	Arg-59	–	1
	Arg-78	–	1
	Val-82	3	–
	Glu-85	–	1
	Gly-89	–	1
	Gly-90	–	1
Mcl-1	Leu-246	–	1
	Met-250	2	–
	Val-253	3	1
	Phe-254	–	1
	Arg-263	1	2
	Leu-267	2	1

Coreximine formed six hydrogen bonds comprising several residues located in BH1 domain namely Leu-246, Leu-267, Phe-254, Val-253 and Arg-263 (Table 4). It also formed eight hydrophobic interactions with Met-250, Val-253, Leu-267 and Arg-263 located in BH1 (Table 4). The binding energy of the interaction was − 7.62 kcal/mol (Table 4). The illustrations were depicted in Fig. 3c, d.

Table 5 The obatoclax interacting residues of the three Bcl-2 antiapoptotic proteins are summarized with the number of hydrophobic interactions and the number of hydrogen bonds

Protein target	Interacting residues	No. of hydrophobic interaction	No. of hydrogen bond
Bcl-2	Phe-109	1	–
	Phe-101	3	–
	Met-112	3	–
	Val-130	1	–
	Leu-134	3	–
	G;y-142	1	–
	Arg-143	3	–
	Ala-146	4	–
	Phe-150	1	–
	Val-153	1	–
Bcl-w	Arg-95	1	–
	Gly-103	–	1
	Tyr-129	2	3
	Leu-134	2	–
	Trp-137	2	–
Mcl-1	Ala-227	2	–
	Phe-228	1	–
	Val-253	2	–
	Thr-266	–	1
	Leu-267	1	1
	Phe-270	1	1
	Gly-271	–	2

MD simulation

Protein model validation

In this study, homology modeling using Phyre2 was employed in order to develop 3D model of the desired protein. Prior to 3D model development, the sequence of desired proteins was retrieved from NCBI database (accession number: Bcl-2 (P10415)). In order to assess the quality of the developed model, several validation tools namely ERRAT, Verify3D and Ramachandran plot analysis were implemented. Referring to the result obtained (Table 6), the 3D protein model generated has passed the evaluation and subjected to structural analysis where the generated 3D protein model was superimposed with its template, 4MAN. As shown in Fig. 4, the overall structure of Bcl-2 protein model is similar to its template (4MAN) with 81.33% identity, thus indicates a good alignment of the two structures.

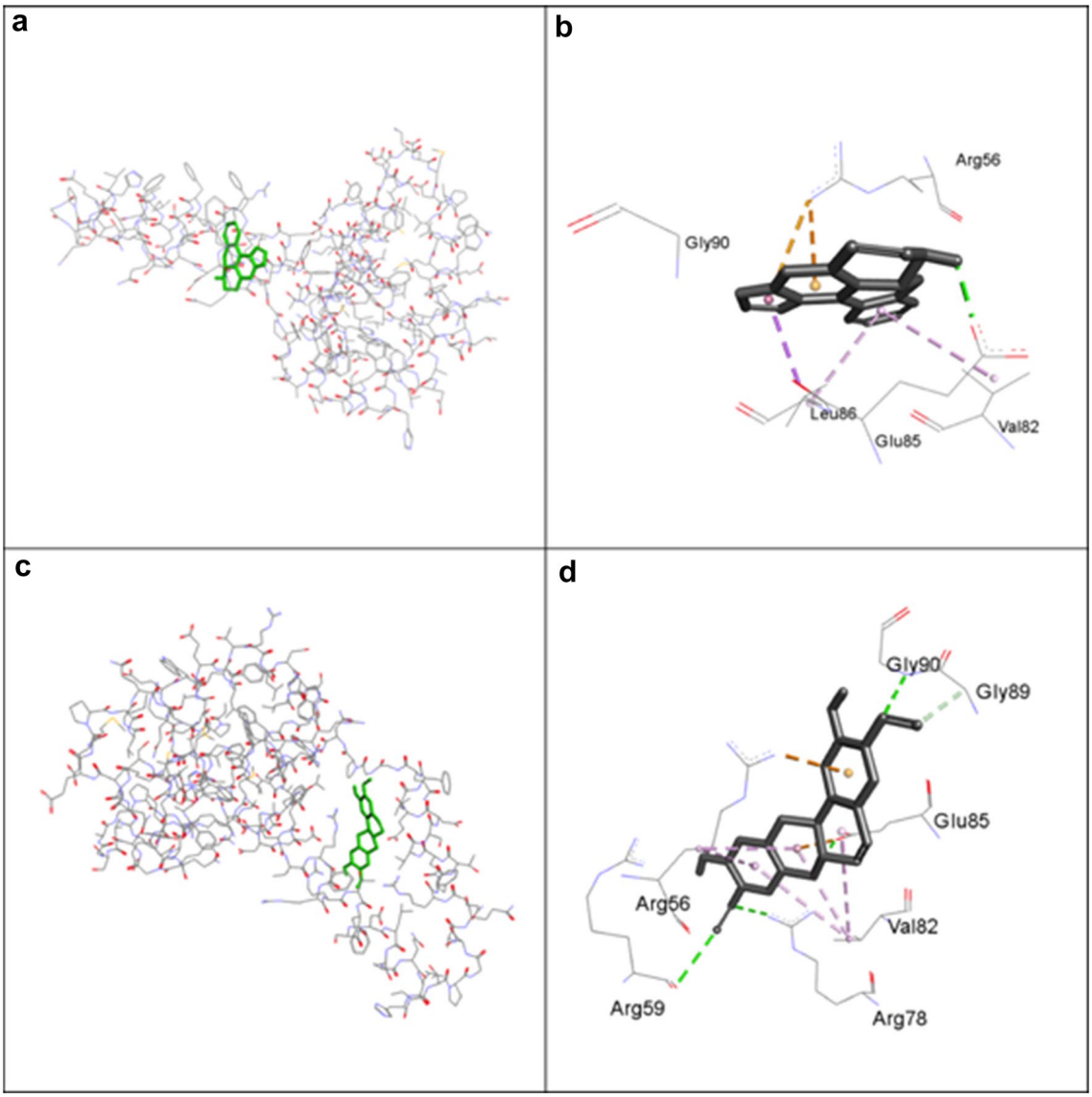

Fig. 2 Binding interactions of anonaine and coreximine in Bcl-w. **a** Representation illustration of anonaine interactions in the hydrophobic pocket of Bcl-w. **b** Hydrophobic interactions of anonaine with residues in the hydrophobic pocket of Bcl-w. **c** Representation illustration of coreximine interactions in the hydrophobic pocket of Bcl-w. **d** Hydrophobic interactions of coreximine with residues in the hydrophobic pocket of Bcl-w

The molecular docking was performed using Autodock 4.2 to generate protein complex of Bcl-2/anonaine and Bcl-2/obatoclax. (Fig. 5a, b).

MD simulation of Bcl-2/obatoclax and Bcl-2/anonaine complex

MD simulation was performed at 310.15 K for 20 ns to determine the stability of Bcl-2 complexes. The RMSD of the resulting trajectories (Fig. 6a) showed that both complexes increased gradually at the initial phase of simulation which indicates the adaptation process of the protein complex with the system. Bcl-2 anonaine remained stable before decreased at 12 ns and increased again towards the end. The average RMSD value for this complex is 0.38. Bcl-2 obatoclax decreased at 5 ns before maintaining considerable pacing until the end of the simulation. The average RMSD value is 0.43. As can be observed from the RMSF graph (Fig. 6b), there are numbers of peaks shown from the beginning until the completion of the simulation. The peaks resulted from the fluctuation that occurred throughout the simulation. The average RMSF value for anonaine complex is 0.16 while obatoclax is 0.17. Meanwhile, the Rg value (Fig. 6c) for both complexes were decreased as the simulation ended at 20 ns, with an average of

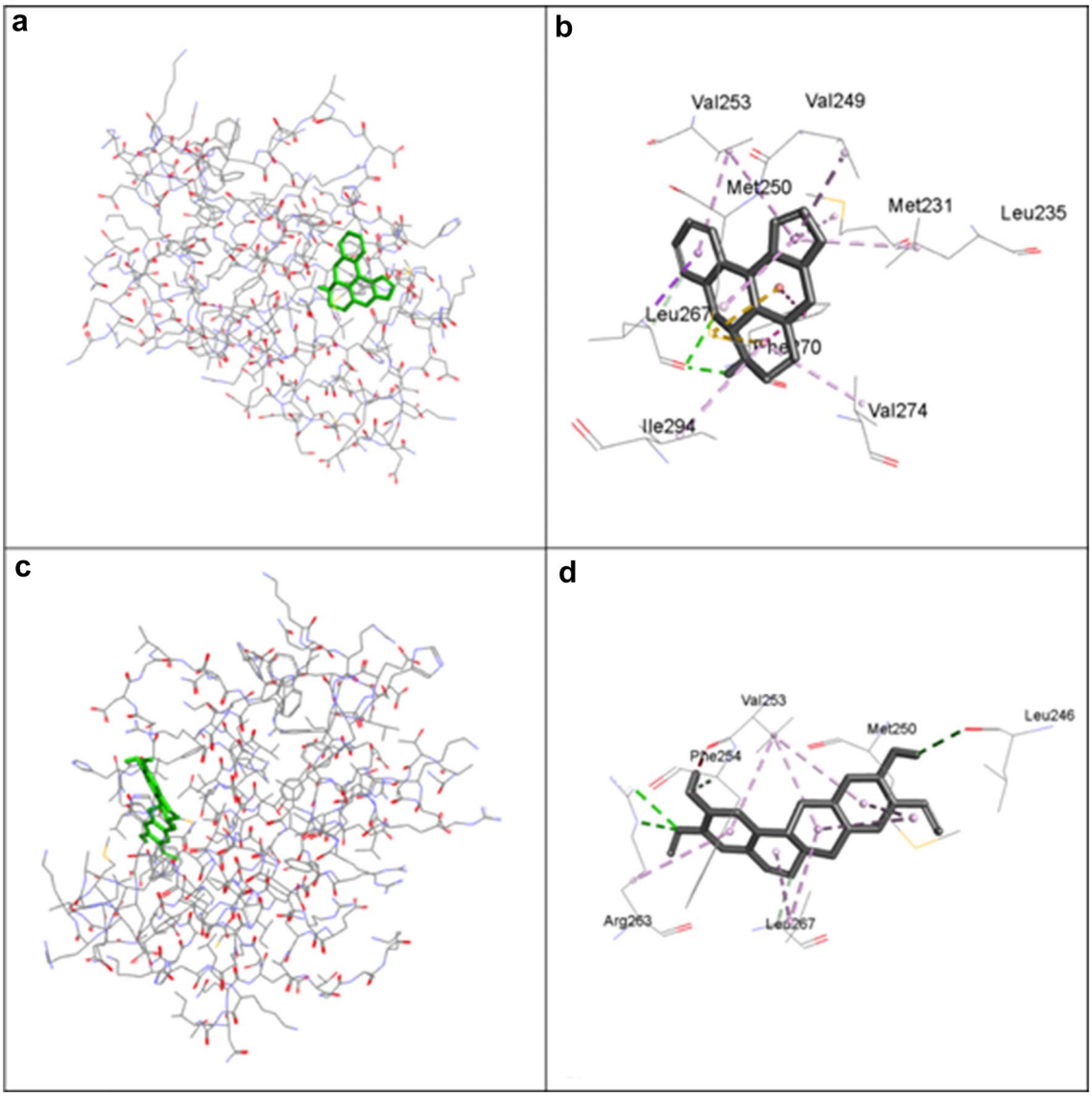

Fig. 3 Binding interactions of anonaine and coreximine in Mcl-1. **a** Representation illustration of anonaine interactions in the hydrophobic pocket of Mcl-1. **b** Hydrophobic interactions of anonaine with residues in the hydrophobic pocket of Mcl-1. **c** Representation illustration of coreximine interactions in the hydrophobic pocket of Mcl-1. **d** Hydrophobic interactions of coreximine with residues in the hydrophobic pocket of Mcl-1

Table 6 Summary of model validation

Evaluation tool	Score (%)	Normal range of score (%)
ERRAT	72.11	> 50
Verify3D	98.19	> 80
Ramachandran plot	97.6	> 90

1.6 and 1.61 for anonaine and obatoclax respectively. Additionally, the SASA analysis (Fig. 6d) was employed for the complexes. It was found that the average SASA value for anonaine complex (105.36) is slightly higher than the obatoclax complex (102.21).

Fig. 4 The superimposition of the generated Bcl-2 protein (blue) and 4MAN protein model template (red) shows high similarity in terms of the protein structure. (Color figure online)

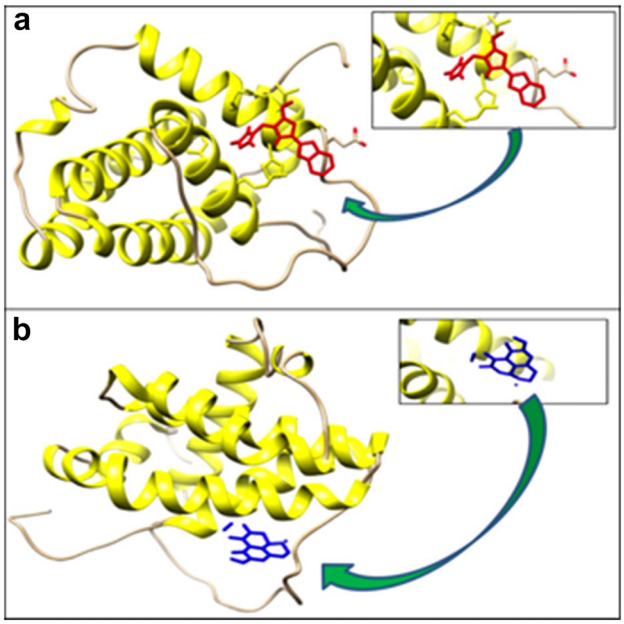

Fig. 5 **a** The structure of Bcl-2 obatoclax protein complex. Red colour structure is the ligand (obatoclax) and the close-up view of the ligand. **b** The structure of Bcl-2 anonaine protein complex. Blue colour structure is the ligand (anonaine) and the close-up view of the ligand. (Color figure online)

Discussion

Potential Bcl-2 antiapoptotic protein inhibitor

Bcl-2 family of antiapoptotic proteins is pivotal in regulating intrinsic mitochondrial apoptotic mechanism. Overexpression of these proteins has been discovered to prevent programmed cell death induced by several stimuli, including hypoxia and oxidative stress [47, 48]. However, it is their ability to inhibit cell death induced by anticancer agents that makes these proteins as potential targets for cancer drug development. Over the past decades, numerous number of Bcl-2 anti-apoptotic proteins inhibitors, especially from natural product, have been developed [49, 50]. For example, bioactive phytochemicals from *A. muricata* L. have been the subjects for the development of antiapoptotic proteins inhibitor in the past few years [51]. Nonetheless, the interactions between these compounds and antiapoptotic proteins remain unclear. Elucidation of the interactions between bioactive compounds of *A. muricata* L. and Bcl-2 antiapoptotic proteins, i.e. Bcl-2, Bcl-w and Mcl-1, will facilitate the development of novel Bcl-2 antiapoptotic proteins inhibitors and may improve currently available cancer treatments.

In this current study, we determined the protein–ligand binding energies and inhibition constants of the interactions, and further characterized the binding amino acid residues involved in the interactions through in silico molecular docking analysis. We found that two bioactive compounds, anonaine and coreximine, demonstrated good affinities with the investigated antiapoptotic proteins, especially Bcl-2, comparable to obatoclax.

Bcl-2 is a major regulator involved in intrinsic mitochondrial apoptotic pathway [9]. Intrinsic mitochondrial apoptotic pathway is a known target in apoptotic signaling and is usually blocked in response to Bcl-2 inhibition [9, 11, 52]. A previous study reported that exogenous inhibition of Bcl-2 by Bcl-2 inhibitor, ABT-199, in its hydrophobic pocket promoted cell death in vitro and antitumor activity in vivo [53]. This is remarkably consistent with our finding that anonaine and coreximine showed good binding affinities towards Bcl-2, forming interactions with hydrophobic residues in binding pocket. Accordingly, we showed that anonaine and coreximine has the ability to interrupt the interaction between proapoptotic and antiapoptotic proteins, thus initiating MOMP and subsequently leading to apoptosis (Fig. 7).

This data is also corroborated with the findings in cell culture analysis by several studies. It has been revealed that anonaine exhibited anticancer activity and cytotoxic activity in several types of cancer cell lines [54, 55]. Anonaine showed antiproliferation activity in cancer cell lines including human cervical (HeLa) cell, hepatocellular carcinoma (HepG2) cell, rodent hepatocytes, and lung malignancy (H1299) cell [54, 55]. In HeLa cell line, anonaine caused DNA damage associated with increased intracellular nitric oxide, reactive oxygen species, MOMP, glutathione depletion, activation of caspase cascade and poly ADP ribose polymerase cleavage [54]. Furthermore, anonaine increased the protein expression of p53 and Bax proteins [54]. Anonaine

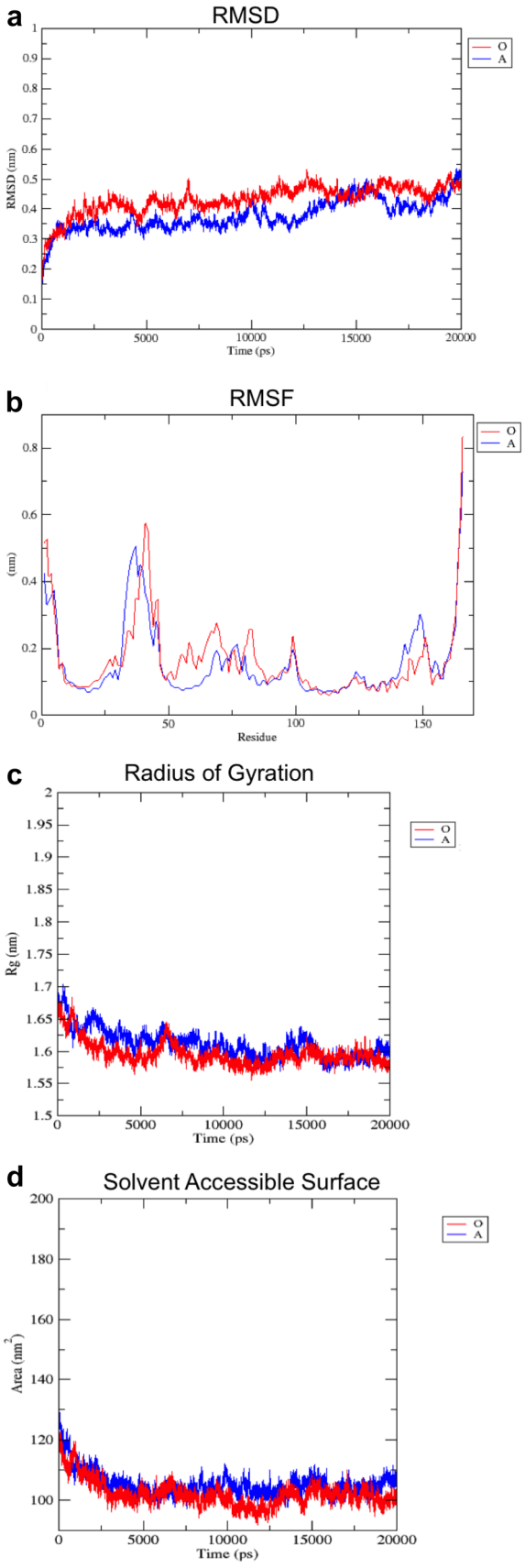

Fig. 6 MD analysis of protein–ligand complex (anonaine and obatoclax) trajectories generated by GROMACS at 310.15 K for 20 ns **a** RMSD; **b** RMSF **c** Rg; **d** SASA. (Anonaine is shown in blue, obatoclax in red). (Color figure online)

played important regulation roles against HepG2 and rodent hepatocyte with IC_{50} estimations of 33.5 and 70.3 µg/mL, respectively [56]. In addition, this compound demonstrated several attributive properties including antiproliferation, antimigration, DNA damage and cell cycle arrest in H1299 [55]. However, there is no record of neither in vitro anticancer study nor in vivo study had been found for coreximine.

An in silico molecular docking study by Antony and Vijayan [51] discovered that bioactive compounds from *A. muricata* L. namely annomuricin A, annohexocin, muricatocin A, annomuricin-D-one and muricatocin A/B displayed high docking score in another antiapoptotic protein, Bcl-Xl, but not in Bcl-2 and Mcl-1 through docking analysis using Schrödinger Glide software. In the current study, we have revealed that annomuricin A demonstrated low affinities against all investigated antiapoptotic proteins. Our model suggested that anonaine and coreximine showed significantly high affinities towards Bcl-2, Bcl-w and Mcl-1 while others compounds including bullatacin, annocatalin, annomuricin A, annomuricin B, annonacin, annonacinone, murisolin and synephrine displayed poor affinities towards these protein targets. Nevertheless, it should be noted that different software would produce different outcomes due to different algorithm applied [51, 57, 58]. On the other hand, different PDB structures used might also contribute to the contrasting outcomes. To overcome these limitations, it is suggested that various PDB structures should be used to represent other experimental models and different software can be used to compare the data. Profiling the bioactive compounds from *A. muricata* L especially anonaine and coreximine against a various number of cancer cell lines are essential for future studies. Furthermore, gene and protein expression analyses of antiapoptotic proteins such as Bcl-2 in these cancer cell lines may elucidate whether the in silico findings can be reflected in both in vitro and in vivo analyses.

Our findings also suggest that hydrophobic pocket, encompassing BH1, BH2 and BH3 domains, is potential site for inhibitory interactions for all three antiapoptotic proteins. In addition, hydrophobic amino acid residues in the hydrophobic pocket are vital for these interactions. These molecular docking results confirmed that bioactive compounds from *A. muricata* L. are potential Bcl-2 antiapoptotic family proteins inhibitors especially for Bcl-2. This study identified and characterized the important amino acid residues involved in the interactions, thus providing preliminary data for Bcl-2 antiapoptotic proteins inhibitors development.

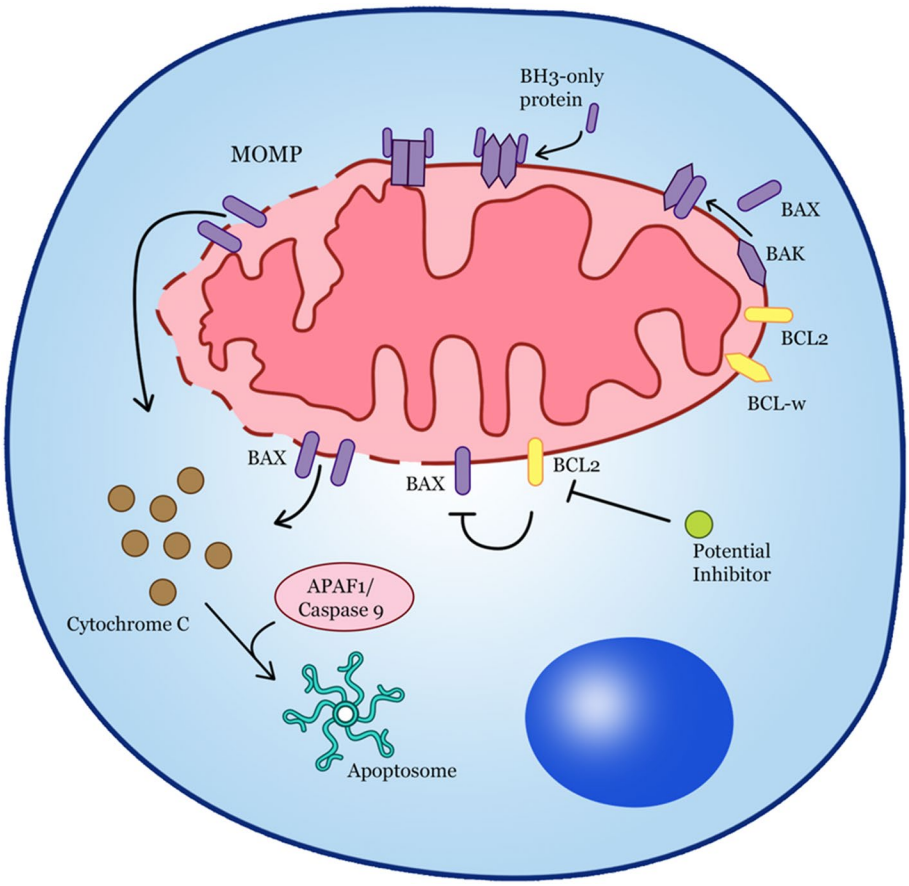

Fig. 7 Potential inhibitory mechanism of action. Inhibition of antiapoptotic proteins such as Bcl-2 by inhibitor liberate proapoptotic proteins (Bax/Bak). Proapoptotic proteins activate the formation of MOMP thus releasing inner mitochondrial membrane contents such as cytochrome c. Release of cytochrome c facilitates the formation of apoptosome containing APAF-1 and caspase 9. This mechanism results in apoptotic machinery

Bcl-2/anonaine complex stability analysis using MD simulation

MD simulation was employed in order to determine the stability of Bcl-2/anonaine complex comparing to Bcl-2/obatoclax complex. The 3D structure of Bcl-2 was generated from Phyre2 and the ligand was docked to this structure. Prior to MD simulation, the 3D structure was validated using several evaluation tools. Firstly, ERRAT was used to determine the quality of the overall structure based on the non-bonded atomic interaction of different atom types which compared to the statistics of highly refined structure. The acceptable range of ERRAT is 50% and above [59]. The ERRAT score of Bcl-2 complex was 72.11, indicating a good quality of protein structure (Table 6). The result of Verify3D for this protein model was excellent with score of 98.19%; Verify3D is an important tool to ensure the compatibility of the 3D model with its amino acid sequence. Finally, Ramachandran plot analysis was carried out to determine the stereochemical quality and accuracy of the protein model. The result showed that 97.6% residues were located in the most favourable and allowed regions. Furthermore, the structural features of the model was further analyzed to ensure that the structure of the 3D model generated is highly compatible with the template. The superimposition of the protein model of Bcl-2 and its template 4MAN (Fig. 1) showed high identity (81.33%) during the superimposition which implies the degree of accuracy of the constructed model. Based on the result obtained using all the aforementioned validation tools, it is very clear that the generated 3D structure is sufficient for MD simulation.

The function of protein is closely related to its structure and dynamics. MD simulation is a great tool which facilitates the study of physical movements of atom and molecules, thus give insights on the protein function. In the present study, the bioactive compound, anonaine showed high binding affinity towards the Bcl-2. Therefore, it would be highly noteworthy to determine the stability of Bcl-2/anonaine complex at its optimum temperature 310.15 K (37 °C). The stability of the resulting trajectories was analyzed based on the changes in RMSD, RMSF, Rg and SASA. The stability of the aforementioned protein complex becomes the interest of this study due to the fact that understanding the factor that contributes to the stability of this complex is vital for the development of Bcl-2 antiapoptotic proteins inhibitor.

RMSD is the measure of average distance between the backbone atoms of protein [60]. As shown in Fig. 6a, the

RMSD value of Bcl-2/anonaine complex is much lower as compared to Bcl-2/obatoclax. According to Esmaili and Shahlaei [61] lower RMSD value corresponds to a much more stable structure. Nevertheless, based on the average RMSD value obtained, it can be observed that both protein complexes are stable at 310.15 K as they possessed good RMSD value of 0.38 and 0.43 respectively. Although RMSD could be a good indicator to estimate structural stability of protein during MD simulation, it is crucial to assess the stability of protein using other analysis as well such as RMSF, Rg and SASA to complement the finding and make it more conclusive and reliable.

RMSF is the measure of flexibility of the system during simulation. It provides an overview of the flexible region of the protein structure. As shown in Fig. (6b), there was not much different in terms of the flexibility of Bcl-2/anonaine and Bcl-2/obatoclax complex. Basically, most of the fluctuated regions in the protein complexes are the loop structure since it is the most flexible part of the protein structure. Theoretically, the higher the RMSF value, the flexible the protein would be, which lessen its stability. The average RMSF value for the protein complexes was in accordance with the RMSD value where the Bcl-2/anonaine complex pictured higher stability as compared to Bcl-2/obatoclax with low RMSD and RMSF value.

Another MD analysis, radius of gyration (Rg) is the measure of compactness for the protein structure. According to Lobanov et al. [62], each of the major class of proteins has its own Rg characteristic which determine the compactness of the protein and later corresponds to its stability. Both protein complexes showed a decrease of Rg value upon the completion of MD simulation (Fig. 6c). The smaller the Rg value indicates better compactness of the protein structure. The difference of 0.01 of Bcl-2/anonaine against Bcl-2/obatoclax complex implied that this bioactive compound was as compact as the preclinical drug. The result of another MD analysis that was closely related with the Rg, SASA, is in agreement with the Rg output. The average SASA value for Bcl-2/anonaine complex (105.36) was slightly higher than obatoclax (102.21). This indicates better contact of Bcl-2/anonaine complex with the environment, which is another indicator for the stability of the protein.

Collectively, the results obtained from MD analysis strongly suggest that protein–ligand complex of Bcl-2/anonaine is comparable with the preclinical drug, obatoclax in terms of the stability.

Conclusion

In summary, the current study explored the interactions of potential bioactive substances of *A. muricata* L. to inhibit Bcl-2 antiapoptotic proteins. The result from this study displayed that anonaine and coreximine demonstrated high affinity towards Bcl-2 antiapoptotic proteins especially Bcl-2 and Mcl-1 comparable to the pre-clinical drug, obatoclax. Interaction analysis revealed that these compounds formed stable interactions in the surface-binding pocket mainly through hydrophobic interactions. Most of these interactions happened through hydrophobic amino acid residues. In addition, MD simulation analysis also reveal that Bcl-2/anonaine complex forms stable complex comparable to Bcl-2/obatoclax complex. Importantly, we systematically provide valuable insights on the identification of potential compounds from *A. muricata* L. in searching for the best selective inhibitors of Bcl-2, Bcl-w and Mcl-1- for cancer treatment. Considering the increased number of experimental therapies targeting Bcl-2-family, our study shed light on the screening of Bcl-2 antiapoptotic proteins inhibitors from plant sources as promising anticancer leads.

Acknowledgements We deeply thank Dr Muhammad Helmi Nadri from Innovation Centre in Agritechnology for Advanced Bioprocessing, Universiti Teknologi Malaysia (UTM-ICA) for valuable comments and suggestions. This work was financially supported by Universiti Teknologi Malaysia and Ministry of Higher Education through Higher Institution Centres of Excellence (HICoE) research Grant (R.J130000.7846.4J261). MNMR was financially supported through Zamalah Scholarship, Universiti Teknologi Malaysia.

References

1. Ferlay J, Soerjomataram I, Ervik M et al. (2013) GLOBOCAN 2012 v1.0, Cancer Incidence and Mortality Worldwide: IARC CancerBase no. 11 [Internet], Lyon, France http://globocan.iarc.fr/Default.aspx Accessed 28 Dec 2015
2. Siegel R, Naishadham D, Jemal A (2012) Cancer statistics, 2012. CA Cancer J Clin 62:10–29. https://doi.org/10.3322/caac.20138
3. Bray F, Jemal A, Grey N et al (2012) Global cancer transitions according to the Human Development Index (2008–2030): a population-based study. Lancet Oncol 13:790–801. https://doi.org/10.1016/S1470-2045(12)70211-5
4. Jemal A, Bray F, Center MM et al (2011) Global cancer statistics. CA Cancer J Clin 61:69–90. https://doi.org/10.3322/caac.20107
5. WHO (2012) Globocan 2012—home. http://globocan.iarc.fr/. Accessed 20 Dec 2016
6. IARC (2016) Globocan 2012. http://www.depiarcfr/Globocan:2012-2013. Accessed 4 Jan 2017
7. Hanahan D, Weinberg RA (2011) Hallmarks of cancer: the next generation. Cell 144:646–674
8. Hanahan D, Weinberg RA (2000) The hallmarks of cancer. Cell 100:57–70

9. Eimon PM, Ashkenazi A (2010) The zebrafish as a model organism for the study of apoptosis. Apoptosis 15:331–349. https://doi.org/10.1007/s10495-009-0432-9
10. Dewson G, Kluck RM (2010) Bcl-2 family-regulated apoptosis in health and disease. Cell Health Cytoskelet 2:9–22. https://doi.org/10.2147/CHC.S6228
11. Cory S, Huang DCS, Adams JM (2003) The Bcl-2 family: roles in cell survival and oncogenesis. Oncogene 22:8590–8607. https://doi.org/10.1038/sj.onc.1207102
12. Sharpe JC, Arnoult D, Youle RJ (2004) Control of mitochondrial permeability by Bcl-2 family members. Biochim Biophys Acta 1644:107–113. https://doi.org/10.1016/j.bbamcr.2003.10.016
13. Adams JM, Cory S (2007) The Bcl-2 apoptotic switch in cancer development and therapy. Oncogene 26:1324–1337. https://doi.org/10.1038/sj.onc.1210220
14. Kim H, Rafiuddin-Shah M, Tu H-C et al (2006) Hierarchical regulation of mitochondrion-dependent apoptosis by BCL-2 subfamilies. Nat Cell Biol 8:1348–1358. https://doi.org/10.1038/ncb1499
15. García-Sáez AJ (2012) The secrets of the Bcl-2 family. Cell Death Differ 19:1733–1740. https://doi.org/10.1038/cdd.2012.105
16. Wei MC, Zong WX, Cheng EH et al (2001) Proapoptotic BAX and BAK: a requisite gateway to mitochondrial dysfunction and death. Science 292:727–730. https://doi.org/10.1126/science.1059108
17. Letai A, Bassik MC, Walensky LD et al (2002) Distinct BH3 domains either sensitize or activate mitochondrial apoptosis, serving as prototype cancer therapeutics. Cancer Cell 2:183–192. https://doi.org/10.1016/S1535-6108(02)00127-7
18. Kuwana T, Bouchier-Hayes L, Chipuk JE et al (2005) BH3 domains of BH3-only proteins differentially regulate Bax-mediated mitochondrial membrane permeabilization both directly and indirectly. Mol Cell 17:525–535. https://doi.org/10.1016/j.molcel.2005.02.003
19. Certo M, Moore VDG, Nishino M et al (2006) Mitochondria primed by death signals determine cellular addiction to antiapoptotic BCL-2 family members. Cancer Cell 9:351–365. https://doi.org/10.1016/j.ccr.2006.03.027
20. Llambi F, Moldoveanu T, Tait SWG et al (2011) A unified model of mammalian BCL-2 protein family interactions at the mitochondria. Mol Cell 44:517–531. https://doi.org/10.1016/j.molcel.2011.10.001
21. Kirkin V, Joos S, Zörnig M (2004) The role of Bcl-2 family members in tumorigenesis. Biochim Biophys Acta Mol Cell Res 1644:229–249. https://doi.org/10.1016/j.bbamcr.2003.08.009
22. Wendt MD (2008) Discovery of ABT-263, a Bcl-family protein inhibitor: observations on targeting a large protein-protein interaction. Expert Opin Drug Discov 3:1123–1143. https://doi.org/10.1517/17460441.3.9.1123
23. Bajwa N, Liao C, Nikolovska-Coleska Z (2012) Inhibitors of the anti-apoptotic Bcl-2 proteins: a patent review. Expert Opin Ther Pat 22:37–55. https://doi.org/10.1517/13543776.2012.644274
24. Baell JB, Huang DCS (2002) Prospects for targeting the Bcl-2 family of proteins to develop novel cytotoxic drugs. Biochem Pharmacol 64:851–863. https://doi.org/10.1016/S0006-2952(02)01148-6
25. Enyedy IJ, Huang Y, Long YQ et al (2001) Discovery of small-molecule inhibitors of Bcl-2 through structure-based computer screening. J Med Chem 44:4313–4324. https://doi.org/10.1021/jm010016f
26. Wang J-L, Liu D, Zhang Z-J et al (2000) Structure-based discovery of an organic compound that binds Bcl-2 protein and induces apoptosis of tumor cells. Proc Natl Acad Sci USA 97:7124–7129
27. Harazono Y, Nakajima K, Raz A (2014) Why anti-Bcl-2 clinical trials fail: a solution. Cancer Metastasis Rev 33:285–294. https://doi.org/10.1007/s10555-013-9450-8
28. Ezirim AU, Okochi VI, James AB, Adebeshi OA, Ogunnowo O (2013) Induction of apoptosis in myelogenous leukemic K562 cells by ethanolic leaf extract of *Annona muricata* L. Glob J Res Med Plants Indig Med 2:142–151
29. Moghadamtousi SZ, Kadir HA, Paydar M et al (2014) *Annona muricata* leaves induced apoptosis in A549 cells through mitochondrial-mediated pathway and involvement of NF-kappa B. BMC Complement Altern Med 14:299. https://doi.org/10.1186/1472-6882-14-299
30. Dayeef AYM, Karyono S, Sujuti H (2013) The influence of *Annona muricata* leaves extract in damaging kidney cell and inducing caspase-9 activity. J Pharm Biol Sci 8:48–52
31. Pieme CA, Kumar SG, Dongmo MS et al (2014) Antiproliferative activity and induction of apoptosis by *Annona muricata* (Annonaceae) extract on human cancer cells. BMC Complement Altern Med 14:516. https://doi.org/10.1186/1472-6882-14-516
32. Dai Y, Hogan S, Schmelz EM et al (2011) Selective growth inhibition of human breast cancer cells by graviola fruit extract in vitro and in vivo involving downregulation of EGFR expression. Nutr Cancer 63:795–801. https://doi.org/10.1080/01635581.2011.563027
33. De Pedro N, Cautain B, Melguizo A et al (2013) Mitochondrial complex i inhibitors, acetogenins, induce HepG2 cell death through the induction of the complete apoptotic mitochondrial pathway. J Bioenerg Biomembr 45:153–164. https://doi.org/10.1007/s10863-012-9489-1
34. Morris GM, Ruth H, Lindstrom W et al (2009) Software news and updates AutoDock4 and AutoDockTools4: automated docking with selective receptor flexibility. J Comput Chem 30:2785–2791. https://doi.org/10.1002/jcc.21256
35. Rizvi SMD, Shakil S, Haneef M (2013) A simple click by click protocol to perform docking: Autodock 4.2 made easy for non-bioinformaticians. EXCLI J 12:830–857
36. Kelly LA, Mezulis S, Yates C et al (2015) The Phyre2 web portal for protein modelling, prediction, and analysis. Nat Protoc 10:845–858. https://doi.org/10.1038/nprot.2015-053
37. Colovos C, Yeates TO (1993) Verification of protein structures: patterns of nonbonded atomic interactions. Protein Sci 2:1511–1519. https://doi.org/10.1002/pro.5560020916
38. Bowie J, Luthy R, Eisenberg D (1991) A method to identify protein sequences that fold into a known three-dimensional structure. Science 253:164–170. https://doi.org/10.1126/science.1853201
39. Lüthy R, Bowie JU, Eisenberg D (1992) Assessment of protein models with three-dimensional profiles. Nature 356:83–85. https://doi.org/10.1038/356083a0
40. Lovell SC, Davis IW, Arendall WB et al (2003) Structure validation by Calpha geometry: phi,psi and Cbeta deviation. Proteins 50:437–450. https://doi.org/10.1002/prot.10286
41. Pettersen EF, Goddard TD, Huang CC et al (2004) UCSF chimera—a visualization system for exploratory research and analysis. J Comput Chem 25:1605–1612. https://doi.org/10.1002/jcc.20084
42. Abraham MJ, Murtola T, Schulz R et al (2015) Gromacs: high performance molecular simulations through multi-level parallelism from laptops to supercomputers. SoftwareX 1–2:19–25. https://doi.org/10.1016/j.softx.2015.06.001
43. Schmid N, Eichenberger AP, Choutko A et al (2011) Definition and testing of the GROMOS force-field versions 54A7 and 54B7. Eur Biophys J 40:843–856. https://doi.org/10.1007/s00249-011-0700-9
44. Schüttelkopf AW, Van Aalten DMF (2004) PRODRG: a tool for high-throughput crystallography of protein-ligand complexes. Acta Crystallogr Sect D Biol Crystallogr 60:1355–1363. https://doi.org/10.1107/S0907444904011679

45. Essmann U, Perera L, Berkowitz ML et al (1995) A smooth particle mesh Ewald method. J Chem Phys 103:8577–8593. https://doi.org/10.1063/1.470117
46. Hess B, Bekker H, Berendsen HJC, Fraaije JGEM (1997) LINCS: a linear constraint solver for molecular simulations. J Comput Chem 18:1463–1472
47. Shimizu S, Eguchi Y, Kamiike W et al (1996) Induction of apoptosis as well as necrosis by hypoxia and predominant prevention of apoptosis by Bcl-2 and Bcl-XL. Cancer Res 56:2161–2166
48. Hockenbery DM, Oltvai ZN, Yin XM et al (1993) Bcl-2 functions in an antioxidant pathway to prevent apoptosis. Cell 75:241–251. https://doi.org/10.1016/0092-8674(93)80066-N
49. Nakashima T, Miura M, Hara M (2000) Tetrocarcin A inhibits mitochondrial functions of Bcl-2 and suppresses its anti-apoptotic activity. Cancer Res 60:1229–1235
50. Huang Z (2000) Bcl-2 family proteins as targets for anticancer drug design. Oncogene 19:6627–6631. https://doi.org/10.1038/sj.onc.1204087
51. Antony P, Vijayan R (2016) Acetogenins from *Annona muricata* as potential inhibitors of antiapoptotic proteins: a molecular modeling study. Drug Des Devel Ther 10:1399–1410. https://doi.org/10.2147/DDDT.S103216
52. Petros A, Olejniczak E, Fesik S (2004) Structural biology of the Bcl-2 family of proteins. Biochim Biophys Acta 1644(2):83–94
53. Souers AJ, Leverson JD, Boghaert ER et al (2013) ABT-199, a potent and selective BCL-2 inhibitor, achieves antitumor activity while sparing platelets. Nat Med 19:202–208. https://doi.org/10.1038/nm.3048
54. Chen CY, Liu TZ, Tseng WC et al (2008) (-)-Anonaine induces apoptosis through Bax- and caspase-dependent pathways in human cervical cancer (HeLa) cells. Food Chem Toxicol 46:2694–2702. https://doi.org/10.1016/j.fct.2008.04.024
55. Chen B-H, Chang H-W, Huang H-M et al (2011) (-)-Anonaine induces DNA damage and inhibits growth and migration of human lung carcinoma h1299 cells. J Agric Food Chem 59:2284–2290. https://doi.org/10.1021/jf103488j
56. Mohamed SM, Hassan EM, Ibrahim N (2010) Cytotoxic and antiviral activities of aporphine alkaloids of Magnolia grandiflora L. Nat Prod Res 24:1395–1402. https://doi.org/10.1080/14786410902906959
57. Meng X-Y, Zhang H-X, Mezei M, Cui M (2011) Molecular docking: a powerful approach for structure-based drug discovery. Curr Comput Aided Drug Des 7:146–157. https://doi.org/10.2174/157340911795677602
58. Plewczynski D, Łaźniewski M, Augustyniak R, Ginalski K (2011) Can we trust docking results? Evaluation of seven commonly used programs on PDBbind database. J Comput Chem 32:742–755. https://doi.org/10.1002/jcc.21643
59. Chaitanya M, Babajan B, Anuradha CM et al (2010) Exploring the molecular basis for selective binding of *Mycobacterium tuberculosis* Asp kinase toward its natural substrates and feedback inhibitors: a docking and molecular dynamics study. J Mol Model 16:1357–1367. https://doi.org/10.1007/s00894-010-0653-4
60. Shamriz S, Ofoghi H (2016) Design, structure prediction and molecular dynamics simulation of a fusion construct containing malaria pre-erythrocytic vaccine candidate, PfCelTOS, and human interleukin 2 as adjuvant. BMC Bioinformatics 17:71. https://doi.org/10.1186/s12859-016-0918-8
61. Esmaili E, Shahlaei M (2015) Analysis of the flexibility and stability of the structure of magainin in a bilayer, and in aqueous and nonaqueous solutions using molecular dynamics simulations. J Mol Model 21:1–15. https://doi.org/10.1007/s00894-015-2622-4
62. Lobanov MI, Bogatyreva NS, Galzitskaia OV (2008) Radius of gyration is indicator of compactness of protein structure. Mol Biol (Mosk) 42:701–706. https://doi.org/10.1134/S0026893308040195